

## Structured Light by Linking Diffraction-Resistant Spatially Shaped Beams

Michel Zamboni-Rached,<sup>1,2,\*</sup> Erasmo Recami,<sup>1,3,4</sup> Tárício A. Vieira,<sup>5</sup> Marcos R.R. Gesualdi,<sup>5</sup> and Jéssyca Nobre-Pereira<sup>1</sup>


<sup>1</sup>*DECOM–FEEC, UNICAMP, Campinas, São Paulo, Brasil*

<sup>2</sup>*University of Toronto, Toronto, Ontario, Canada*

<sup>3</sup>*Facoltà di Ingegneria, Università statale di Bergamo, Dalmine, Bergamo, Italy*

<sup>4</sup>*INFN—Sezione di Milano, Milan, Italy*

<sup>5</sup>*CECS, Federal University of ABC, Santo André, São Paulo, Brazil*

 (Received 7 November 2017; revised manuscript received 23 March 2018; published 12 September 2018)

We present a theoretical method, together with its experimental confirmation, to obtain structures of light by connecting diffraction-resistant cylindrical beams of finite lengths and different radii. The resulting “LEGO-like beams” can assume, on demand, various unprecedented spatial configurations. We also experimentally generate some of them using a computational holographic technique and a spatial light modulator. Our method of linking together various *pieces of light* can find applications in all fields where structured light beams are needed, in particular, optical tweezers (e.g., for biological manipulations), optical guiding of atoms, control of orbital angular momentum of light, holography, lithography, nonlinear optics, and interaction of electromagnetic radiation with Bose-Einstein condensates, besides, in general, the field of localized waves (nondiffracting beams and pulses).

DOI: [10.1103/PhysRevApplied.10.034023](https://doi.org/10.1103/PhysRevApplied.10.034023)

### I. INTRODUCTION

Structured light [1–6] is being studied more and more, and is being applied in various fields, such as optical tweezers [7–17], optical guiding of atoms [18–24], imaging [25], control of orbital angular momentum of light and its applications [26–31], and photonics in general.

A rather efficient method to model longitudinally the intensity of nondiffracting beams is by the use of so-called frozen waves (FWs) [1–3,32–36] obtained from superpositions of copropagating Bessel beams with the same frequency and order. The resulting diffraction-resistant beam, with a longitudinal intensity shape freely chosen *a priori*, may then propagate, remaining confined, along the propagation axis  $z$ , or over a cylindrical surface (depending on the order of the constituting Bessel beams), while its “spot” size and the cylindrical surface radius can also be chosen *a priori*. In this way, it is possible to construct, for example, cylindrical beams whose static envelopes possess non-negligible energy density in finite, well-defined spatial intervals only, so they can be regarded as *segments or cylindrical pieces of light*.

Aiming also at greater control of the *transverse* shape of the beam, another method was recently proposed [24,26] where different-order FW-type beams are superposed that

possess appreciable intensities along different, but consecutive, space intervals, resulting in cylindrical structures of light with different radii and located at different positions along the  $z$ -axis. This new method is efficient also for controlling the orbital angular momentum along the propagation axis [26].

It is possible to join in the same way even two FW-type beams of the *same order* by creating again a structure with two cylinders of different radii, each in its own space interval. To this aim, it is sufficient that each equal-order FW has a different value of its central longitudinal wave number, which implies a different radius for the corresponding cylindrical structure. An advantage of using FWs of the same order is that the resulting beam intensity keeps its azimuthal symmetry, thus avoiding the intensity perturbations (asymmetries) that one meets on the transverse plane where two different-order FWs connect to each other.

In this work we extend—theoretically and experimentally—a method of ours proposed in Refs. [24,26] by explicitly considering superpositions not only of different-order FWs but also of FWs of the same order but with different central longitudinal wave numbers. Moreover, we also investigate the superposition of FWs whose longitudinal intensities are nonzero inside the *same* space interval. This allows us to create coaxial light structures, cylindrical structures [e.g., with “emboli” (blockages)], and so on.

We call all such structures of light “LEGO-like beams.” Our method of linking together various “pieces of light”

\*mzamboni@decom.fee.unicamp.br;  
michelunicamp@yahoo.com.br

can find applications in all fields where structured light beams are needed, such as, in particular, optical tweezers (e.g., for biological manipulations), optical guiding of atoms, control of orbital angular momentum of light, holography, lithography, nonlinear optics, and interaction of electromagnetic radiation with Bose-Einstein condensates, besides, of course, the field of localized waves (nondiffracting beams and pulses).

## II. THE METHOD

Let us consider as an exact solution to the wave equation the following superposition:

$$\Psi(\rho, \phi, z, t) = \sum_{\nu=-\infty}^{\infty} \sum_{\ell=-\infty}^{\infty} \psi_{\nu\ell}(\rho, \phi, z, t), \quad (1)$$

with

$$\psi_{\nu\ell}(\rho, \phi, z, t) = \mathcal{M}_\nu \sum_{n=-N_{\nu\ell}}^{N_{\nu\ell}} A_{\nu\ell n} J_\nu(h_{\nu\ell n} \rho) e^{i\nu\phi} e^{\beta_{\nu\ell n} z}, \quad (2)$$

where

$$\beta_{\nu\ell n} = Q_{\nu\ell} + \frac{2\pi}{L} n, \quad (3)$$

$$h_{\nu\ell n} = \sqrt{k^2 - \beta_{\nu\ell n}^2}, \quad (4)$$

$$A_{\nu\ell n} = \frac{1}{L} \int_0^L F_{\nu\ell}(z) e^{-i(2\pi/L)nz} dz, \quad (5)$$

$k = \omega/c$ , and  $\mathcal{M}_\nu = 1/[J_\nu(\cdot)]_{\max}$ , with  $[J_\nu(\cdot)]_{\max}$  being the maximum value of the  $\nu$ -order Bessel function of the first kind. In Eq. (5),  $F_{\nu\ell}(z)$  are freely chosen functions that are related to the desired longitudinal intensity patterns of  $\psi_{\nu\ell}(\rho, \phi, z, t)$ , as we will see later.

For better understanding of the method, we explicitly examine the main solution given by Eq. (1). First, let  $\nu$  and  $\ell$  have fixed values, and then consider a term  $\psi_{\nu\ell}(\rho, \phi, z, t)$  of the series. Equation (2) reveals that such a term is a FW [1–3] of order  $\nu$  whose central longitudinal wave number ( $n = 0$ ) is  $\beta_{\nu\ell 0} = Q_{\nu\ell}$ , so  $h_{\nu\ell 0} = \sqrt{k^2 - Q_{\nu\ell}^2}$ , and the FW intensity shape  $|F_{\nu\ell}(z)|^2$  in the interval  $0 \leq z \leq L$  is concentrated (i) either on a cylindrical surface with radius  $\rho_\nu \approx s_\nu/h_{\nu\ell 0}$  [ $s_\nu$  being the value of  $s$  where  $J_\nu(s)$  is maximum] in the case  $\nu \geq 1$  or (ii) around the propagation axis  $z$ , with a spot radius  $r_0 \approx 2.4/h_{0\ell 0}$ , in the case  $\nu = 0$ . Here, we define  $\rho_0 \equiv 0$ . In any case,  $|\psi_{\nu\ell}(\rho = \rho_\nu, \phi, z, t)|^2 \approx |F_{\nu\ell}(z)|^2$ .

We now examine the sum  $\sum_\ell \psi_{\nu\ell}$  in Eq. (1). It represents a superposition of FWs of the same order  $\nu$ , but with

different values of their central longitudinal wave numbers  $\beta_{\nu\ell 0} = Q_{\nu\ell}$ . Each FW (of the same order but with different  $\ell$ ) has its own longitudinal intensity shape  $|F_{\nu\ell}(z)|^2$ .

Finally, the last sum (i.e.,  $\sum_\nu \sum_\ell \psi_{\nu\ell}$ ) refers to superposition of *different-order* FWs. As before, for each  $\nu$  we deal with FWs with different values of  $\ell$  (i.e., with different values of  $Q_{\nu\ell}$  for their central longitudinal  $\beta_{\nu\ell 0}$ ) and also with their own longitudinal intensity shapes.

Before continuing, we stress the type of light structures that can be properly built by the solution we started from. We know that each  $\psi_{\nu\ell}$  in the superposition represented by Eq. (1) is a FW whose *static intensity envelope* can be regarded as a “piece” of light. Because of the interference present in any wave phenomena, when summing different FWs together, such as  $\psi_1$  and  $\psi_2$ , one does not obtain the mere sum of their intensity envelopes. For instance,

$$|\psi_1 + \psi_2|^2 = |\psi_1|^2 + |\psi_2|^2 + 2|\psi_1||\psi_2| \cos \delta, \quad (6)$$

where  $\delta$  is the phase difference between the two waves. To minimize the contribution associated with these phase differences, one has to avoid, for example, cases in which two different FWs have relevant intensities in the same spatial region. We can choose, for instance, different FWs,  $\psi_{\nu\ell}$ , that in the region  $0 \leq z \leq L$  have appreciable longitudinal intensity patterns,  $|F_{\nu\ell}(z)|^2$ , only in different, and consecutive, intervals. Even when the interference is minimized, it continues to exist, its critical effect being in the welding region. In other words, critical interference occurs in the  $z$ -planes corresponding to the interval boundaries. A way to avoid this is to choose successive FWs with orthogonal polarizations so that the double-type product [as that in Eq. (6)] is absent. This will be examined in future work.

It is also possible to obtain interesting light structures by superposing FWs with nonzero intensities over the same  $z$ -interval, provided that the corresponding cylindrical structures have *rather different radii*, thus obtaining interesting coaxial structures for light.

Everything is made clearer by the theoretical and experimental examples presented in the next sections.

## III. THEORETICAL EXAMPLES

In this section we apply our method to obtain some interesting *structured* optical beams. We adopt a frequently used wavelength:  $\lambda = 632.8$  nm.

We describe in enough detail our *first example* of a LEGO-like beam; namely, a beam whose spatial structure consists of two adjacent cylindrical surfaces, 12 and 16 cm long, with corresponding radii of 128 and 182  $\mu\text{m}$  subsequently linked to each other, and a coaxial, central light segment having a spot size of 15  $\mu\text{m}$  and length of 28 cm.

To obtain such a beam, we use our solution, Eq. (1), and consider only three FWs, one of order 0 and the other two of order 10 (but with different values of their central

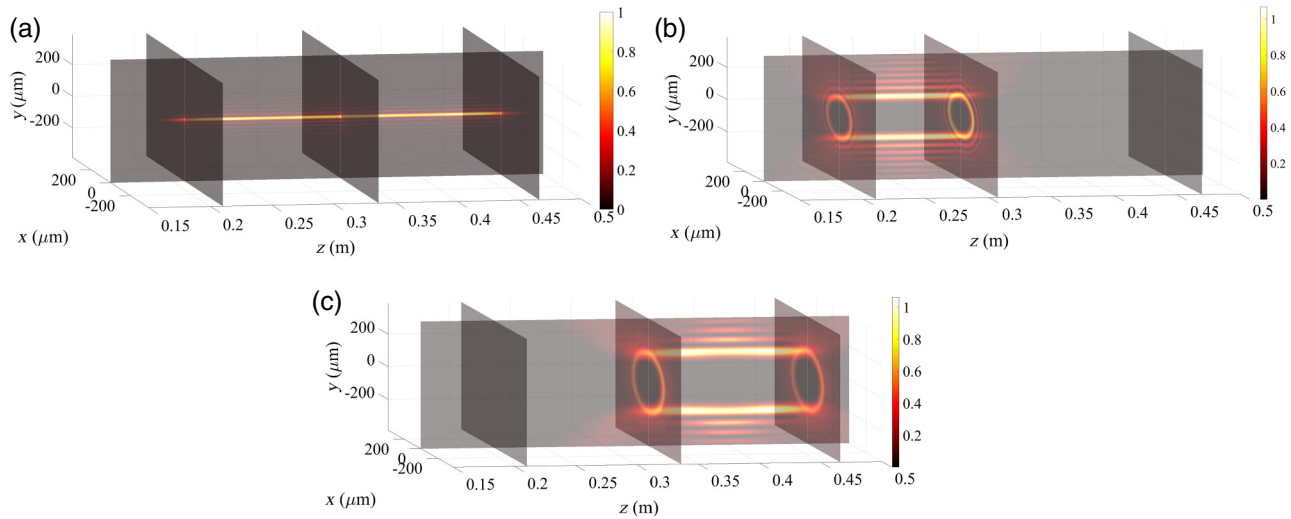


FIG. 1. The intensities of the three FWs that compose our beam (in a sense, the pieces of the LEGO-like beam are shown).

longitudinal wave numbers). That is, we do this by inserting in Eq. (1) the nonzero functions (FWs)  $\psi_{00}$ ,  $\psi_{100}$ , and  $\psi_{101}$  having in the interval  $0 \leq z \leq L = 1$  m the longitudinal intensity shapes,  $|F_{\nu\ell}(z)|^2$ , dictated by the following morphological function:

$$\begin{aligned}
 F_{\nu\ell}(z) = & \delta_{\nu 0} \delta_{\ell 0} [H(z - 0.2) - H(z - 0.48)] \\
 & + 0.8 \delta_{\nu 10} \delta_{\ell 0} [H(z - 0.2) - H(z - 0.325)] \\
 & + 0.8 \delta_{\nu 10} \delta_{\ell 1} [H(z - 0.32) - H(z - 0.48)], \quad (7)
 \end{aligned}$$

where  $\delta_{pq}$  is the Kronecker  $\delta$  function and  $H(\cdot)$  is the Heaviside function. The corresponding  $Q_{\nu\ell}$  are evaluated on the basis of the desired values for the cylindrical surface radii and the light-segment spot, resulting in

$$\begin{aligned}
 Q_{00} &= 0.9999100 \frac{\omega}{c}, \\
 Q_{100} &= 0.9999700 \frac{\omega}{c}, \\
 Q_{101} &= 0.9999850 \frac{\omega}{c}.
 \end{aligned} \quad (8)$$

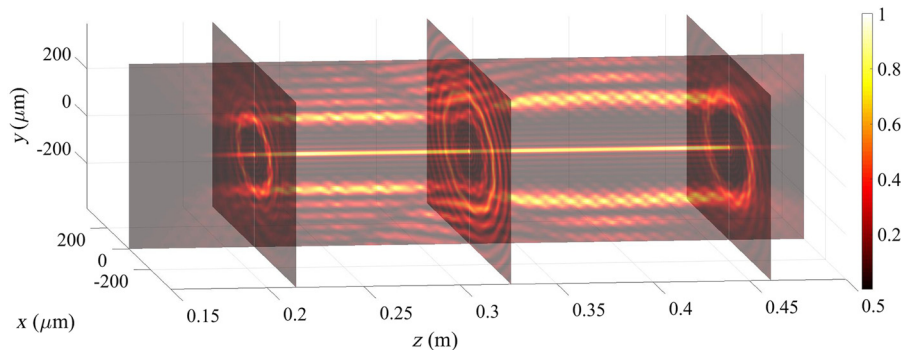


FIG. 2. The intensity of the resulting beam (i.e., the intensity of the structured light resulting from the sum of the FWs chosen).

Then the coefficients  $A_{\nu\ell n}$  can be easily obtained via Eq. (5), and the longitudinal and transverse wave numbers,  $\beta_{\nu\ell n}$  and  $h_{\nu\ell n}$ , respectively, are obtained by Eqs. (3) and (4). In the present example, it is sufficient to use 25 Bessel beams in each of the FWs considered; that is,  $N_{\nu\ell} = 12$ .

Our results are shown in Figs. 1 and 2. Figure 1 shows the intensities of the three FWs that compose our beam (in a sense, the pieces constituting the resulting beam are shown). Figure 2 shows the intensity of the resulting beam (i.e., the intensity of the structured light resulting from the sum of the FWs chosen).

One can see that the interferences among the three FWs are minimized because such FWs have relevant intensities in different space regions.

We show some further possibilities provided by our method, even if—for the sake of conciseness—we skip the mathematical details. We show in Fig. 3 four further light structures obtained from Eq. (1).

Figure 3(a) depicts the intensity of the resulting beam consisting of two cylindrical surfaces of different (decreasing) radii linked to each other, with the cylinder on the right side having a light segment acting as a “cork.” Figure 3(b) shows the intensity of a structured light beam

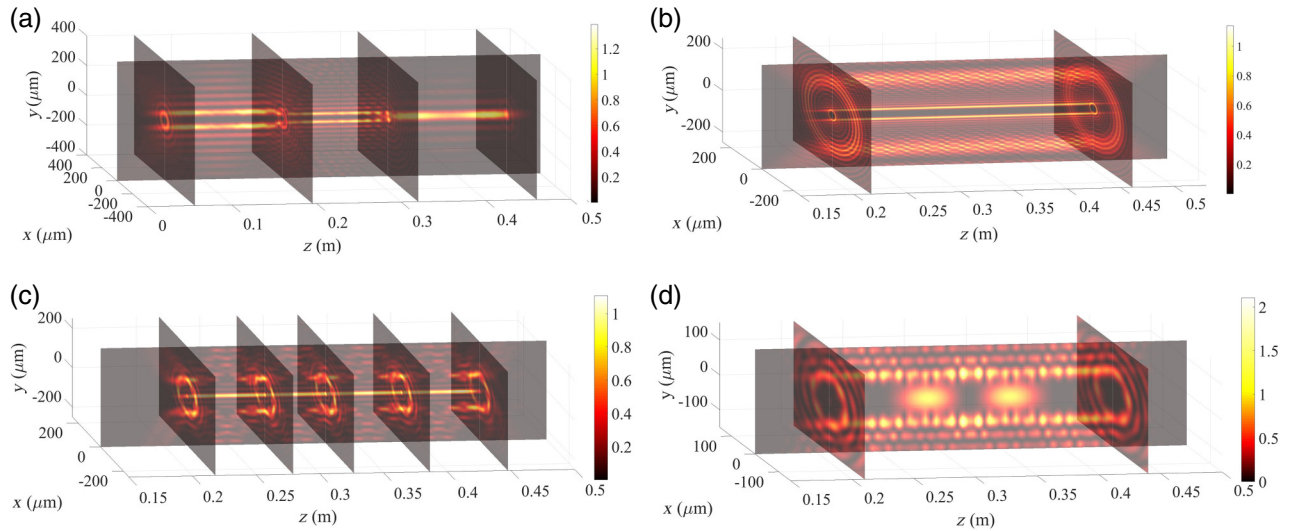


FIG. 3. Four further interesting beams obtained by our method. They refer to cylindrical or threadlike structures (adjacent or coaxial in their location), having transverse sizes of tens of micrometers and longitudinal sizes of tens of centimeters. They are, therefore, highly resistant to diffraction effects. See also the text.

formed from two coaxial cylindrical surfaces. In this case two FWs of the same order (larger than zero, of course) are used. Figure 3(c) shows a sequence of donut-shaped light structures, with a central coaxial (zeroth-order) light line. Figure 3(d) shows the intensity of a structured beam made of a cylindrical surface with two light “emboli” (blockages) inside it.

All these examples refer to cylindrical or threadlike structures (adjacent or coaxial in their location), having transverse sizes of tens of micrometers and longitudinal sizes of tens of centimeters. They are, therefore, highly resistant to diffraction effects.

#### IV. EXPERIMENTAL CONFIRMATION

We present a couple of experimental confirmations of our approach by constructing two LEGO-like beams via a holographic setup that performs the optical reconstruction of computer-generated holograms (CGHs) sent electronically into a reflective spatial light modulator (SLM), used in amplitude-modulation mode, followed by a 4F spatial filtering system. Further details can be found in the caption of Fig. 4.

We obtain the two-dimensional CGH through the complex transmittance function (hologram) obtained from the desired resulting beam at the origin  $\Psi(\rho, \phi, z = 0, t)$ , with  $\Psi$  given by Eq. (1). The hologram equation is expressed as [32,33,37,38]

$$H(x, y) = \frac{1}{2} \{ \beta(x, y) + \alpha(x, y) \cos[\theta(x, y) - 2\pi(u_0x + v_0y)] \}, \quad (9)$$

where  $\alpha(x, y)$  and  $\theta(x, y)$  are the amplitude and phase, respectively, of the complex field  $\Psi(\rho, \phi, z = 0, t)$ ,  $\beta(x, y) = [1 + \alpha^2(x, y)]/2$  being a bias function chosen as a soft envelope for the amplitude  $\alpha(x, y)$ . To make easier the separation of the different diffraction orders from the encoded complex field  $\Psi(\rho, \phi, z, t)$ , the off-axis reference plane wave  $\exp[i2\pi(\xi x + \eta y)]$  is used, shifting, in the Fourier plane, the center of signal information to the spatial frequencies  $u_0$  and  $v_0$ .

The holographic setup used in the experimental reconstruction of the CGH is shown in Fig. 4. The coherent light from a He-Ne laser (632.8 nm) passes through the spatial filter SF and is collimated by lens L1; it is then reflected by mirror M1 and polarized by polarizer P1. When it arrives at

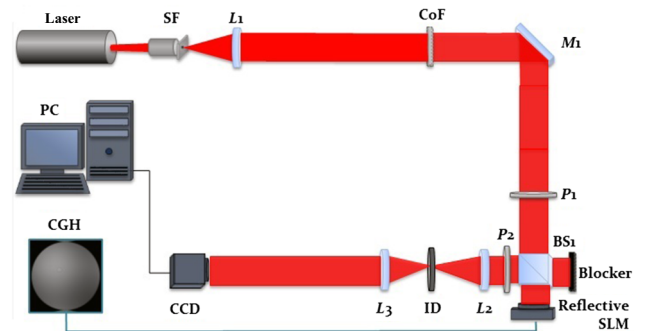


FIG. 4. The holographic setup used in experimentally reconstructing the CGHs of the LEGO-like beams. A He-Ne laser (632.8 nm) is used. SF is a spatial filter; L1, L2, and L2 are lenses; CoF is a neutral-density filter; M1 is a mirror; P1 and P2 are polarizers; BS1 is a beam splitter; ID is an iris diaphragm; and CCD is a camera.



the beam splitter BS1, the light is directed to the reflective SLM (model LC-R 1080, Holoeye Photonics), to where the CGH was sent electronically, and diffracted, proceeding to polarizer P2. To select the correct diffraction order of the reconstructed (diffracted) beam, a 4F filter is used after the SLM, composed of two lenses (L2 and L3) and an iris diaphragm ID. Finally, the desired beam is acquired by the CCD camera (model DMK 41BU02.H, Imaging Source) at subsequent locations along  $z$ .

The first experimentally generated beam has a shape similar to that of the first theoretical example, but with different values for the radii of the cylindrical surfaces due to the limited resolution of our SLM. Namely, we generate a beam whose diffraction-resistant spatial structure consists of two adjacent cylindrical surfaces, 12 and 16 cm long, with corresponding radii of 148 and 203  $\mu\text{m}$ , sequentially linked to the other, while coaxially there is a “light segment” having a spot of 38  $\mu\text{m}$  and a length of 28 cm.

We use, therefore, our main solution, Eq. (1), with three FWs: one zeroth-order FW, and two eighth-order FWs (the latter have different values of the central longitudinal wave numbers). That is, in Eq. (1) the nonzero functions (FWs)  $\psi_{v\ell}$  are  $\psi_{00}$ ,  $\psi_{80}$ , and  $\psi_{81}$ , having in the interval  $0 \leq z \leq L = 0.6$  m the longitudinal intensity shapes,  $|F_{v\ell}(z)|^2$ , dictated by

$$\begin{aligned} F_{v\ell}(z) = & 1.2\delta_{v0}\delta_{\ell0}[H(z - 0.2) - H(z - 0.48)] \\ & + \delta_{v8}\delta_{\ell0}[H(z - 0.2) - H(z - 0.32)] \\ & + 1.1\delta_{v8}\delta_{\ell1}[H(z - 0.32) - H(z - 0.48)], \quad (10) \end{aligned}$$

where  $\delta_{pq}$  is a Kronecker  $\delta$  function and  $H(\cdot)$  is a Heaviside function. The corresponding  $Q_{v\ell}$  values depend on the cylindrical surface radii chosen and on the light-segment spot, resulting in

$$\begin{aligned} Q_{00} &= 0.9999800 \frac{\omega}{c}, \\ Q_{80} &= 0.9999785 \frac{\omega}{c}, \\ Q_{81} &= 0.9999885 \frac{\omega}{c}. \end{aligned} \quad (11)$$

Again, coefficients  $A_{v\ell n}$  are evaluated via Eq. (5), while the longitudinal values,  $\beta_{v\ell n}$ , and the transverse ones,  $h_{v\ell n}$ , of the wave numbers are given by Eqs. (3) and (4). For the number of terms  $N_{v\ell}$  for each  $\psi_{v\ell}$ , we use  $N_{00} = 14$ ,  $N_{80} = 10$ , and  $N_{81} = 10$ , respectively.

Figure 5 shows the experimentally generated beam. At the top, the theoretical prediction is shown. Excellent agreement is apparent, which confirms the validity and applicability of our method.

We now consider the second experimentally generated LEGO-like beam. We choose two coaxial cylindrical light surfaces, in analogy to our theoretical situation in Fig. 3(b), where we use two equal-order FWs (while for the experiment we use two different-order FWs). More specifically, we want to generate two coaxial light surfaces having the same length 20 cm but different radii of 45 and 360  $\mu\text{m}$ . In other words, we now adopt the main solution, Eq. (1), with two FWs only, the first of order 2 and the second of order 22. Therefore, in Eq. (1) and in the interval  $0 \leq z \leq$

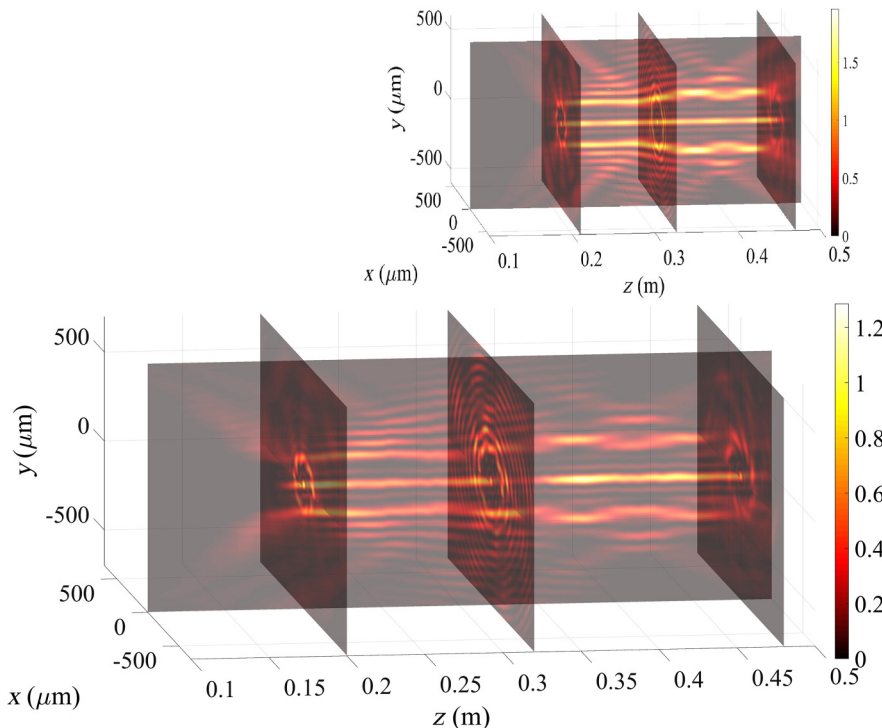


FIG. 5. Intensity of the first LEGO-like beam generated experimentally, whose diffraction-resistant spatial structure consists of two adjacent cylindrical light surfaces, 12 and 16 cm long, with corresponding radii of 148 and 203  $\mu\text{m}$ , sequentially linked to each other. Coaxially there is a “light segment” having a spot of 38  $\mu\text{m}$  and a length of 28 cm. The corresponding theoretical prediction is shown at the top.

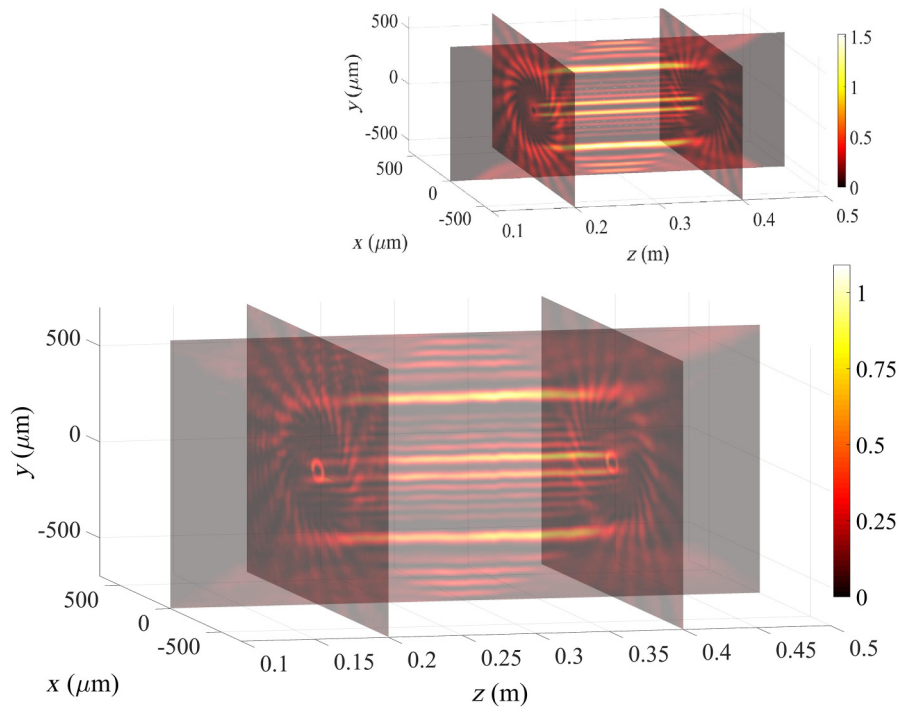


FIG. 6. Intensity of the second LEGO-like beam generated experimentally. This beam is composed of two coaxial cylindrical light surfaces having the same length of 20 cm but the different radii of 45 and 360  $\mu\text{m}$ . The corresponding theoretical prediction is shown at the top.

$L = 0.5$  m, the nonzero functions (FWs)  $\psi_{v\ell}$  are  $\psi_{20}$  and  $\psi_{220}$ , whose longitudinal intensity patterns,  $|F_{v\ell}(z)|^2$ , are dictated by

$$F_{v\ell}(z) = \delta_{v2}\delta_{\ell0}[H(z - 0.2) - H(z - 0.4)] + \delta_{v22}\delta_{\ell0}[H(z - 0.2) - H(z - 0.4)], \quad (12)$$

where, again,  $\delta_{pq}$  is a Kronecker  $\delta$  function and  $H(\cdot)$  is a Heaviside function. The corresponding  $Q_{v\ell}$  values, depending on the cylindrical surface radii chosen, are

$$Q_{20} = Q_{220} = 0.9999770 \frac{\omega}{c}. \quad (13)$$

As before, coefficients  $A_{v\ell n}$  are evaluated via Eq. (5), and the longitudinal and transverse wave numbers ( $\beta_{v\ell n}$  and  $h_{v\ell n}$ ) are calculated by Eqs. (3) and (4). For this example we use  $N_{20} = N_{220} = 18$ .

Figure 6 shows this second experimentally generated beam and at the top the theoretical prediction is shown. Once more, excellent agreement is found between theory and experiment, provided our discussion of the interference between different FWs at the end of Sec. II is kept in mind.

In connection with Fig. 6 and with Eq. (6), we add a particular comment: if the external cylinder stays in the region where  $\cos \delta$  is positive (negative), in the resulting beam its intensity will be higher (lower) than the internal cylinder's. Such effects can be avoided, or at least reduced, by the proper choice of the (greater or smaller) intensities of the initial cylinders so that in the final beam they have the same intensity.

## V. CONCLUSIONS

We present a theoretical method in which FW-type optical beams (of different orders and/or with different sets of longitudinal wave numbers) are suitably superposed, providing us with really innovative possibilities (which we call “LEGO-like beams”) in the important field of structured light.

Various theoretical examples are developed and, moreover, our method is experimentally verified by the production of two such beams via a holographic setup that performs the optical reconstruction of CGHs through a reflective SLM followed by a 4F spatial filtering system.

The study of structured light has played an important role in several areas of optics and photonics, and our present results can find interesting applications in all sectors in which more sophisticated light beams are needed, such as optical tweezers, optical guiding of atoms, control of orbital angular momentum light, imaging systems, remote sensing, light detection and ranging, microscopy, metrology, optical communications, and quantum information. All these technologies are growing and mastering the various types of structured light is becoming more and more important [39].

For completeness, we specify in more detail the expected applications of the beams presented here:

- (i) Optical tweezers are a highly valuable instrument for confining and manipulating nanoparticles or microparticles, including biological “particles” such as bacteria, cells, and viruses. The use of nondiffracting beams resulted in many improvements [8–17], to the point where it was

regarded as revolutionary [13]. Among their advantages, is the possibility of simultaneously trapping many scatterers. The ability to spatially model nondiffracting beams, as presented here, is certainly useful for optical micro-manipulations, generating new light structures that could not be imagined before. For instance, by linking together a zeroth-order FW (devoid of orbital angular momentum) and a FW of order 1 or more (with orbital angular momentum), one can create a confining region wherein the particles do not receive angular momentum, followed by another confining region in which the particles get angular momentum from the optical field and start rotating.

(ii) Another sector where the use of nondiffracting beams is useful and promising is the optical guiding of neutral atoms, when Bessel beams of order larger than zero (nondiffracting hollow beams) generate optical potentials with the same shape [18–24]. Again, the possibility of obtaining diffraction-resistant beams with various interesting, new spatial configurations (by connecting different FWs together) can lead to unprecedented optical potential configurations for guiding, or holding, neutral atoms.

(iii) Applications in material modification, more specifically the creation of waveguide structures and microchannels for microfluidics through the process of laser-writing, where a femtosecond laser induces a material modification (e.g., refractive index modification) in the longitudinal direction. Good results for laser micromachining in glass with Bessel beams have been reported [40–43], with microchannels with a diameter of  $2\ \mu\text{m}$  and with high aspect ratios (up to 40) being obtained. The beams developed here could be used for laser-writing waveguide structures and microchannels (for microfluidics) with a great variety of forms and, because of their diffraction-resistant characteristics, with long longitudinal lengths.

(iv) A fourth interesting sector is that of examining (theoretically and experimentally) the interaction of the beams presented here with Bose-Einstein condensates. The Gross-Pitaevskii equation—describing a weakly interacting Bose-Einstein condensate at the limit of zero temperature—has a mathematical structure similar to that of the nonlinear Schrödinger equation in optics. Such a mathematical equivalence suggests that, while in the nonlinear Schrödinger equation light is the wave propagating in a medium constituted of atoms, in the Gross-Pitaevskii equation the atoms play the role of the wave (matter wave) and light acts as the propagation medium [44]. It is tempting, in this context, to investigate in theory and experiments the effect of such structured beams on those condensates.

#### ACKNOWLEDGMENTS

This work was supported by FAPESP (Grants No. 2015/26444-8 and No. 16/19131-6), CNPq (Grants No. 304718/2016-5 and No. 313153/2014-0), and CAPES.

E.R. received support from a CAPES Visiting Professor Fellowship c/o UNICAMP. The authors also thank Mo Mojahedi, Ahmed H. Dorrah, and Hugo E. Hernández-Figueroa for their continuous collaboration and interest.

- 
- [1] M. Zamboni-Rached, Stationary optical wave fields with arbitrary longitudinal shape by superposing equal frequency Bessel beams: Frozen Waves, *Opt. Express* **12**, 4001 (2004).
  - [2] Michel Zamboni-Rached, Diffraction-attenuation resistant beams in absorbing media, *Opt. Express* **14**, 1804 (2006).
  - [3] M. Zamboni-Rached, E. Recami, and H. E. Hernández-Figueroa, Theory of ‘frozen waves’: Modeling the shape of stationary wave fields, *J. Opt. Soc. Am. A* **22**, 2465 (2005).
  - [4] *Localized Waves*, edited by H. E. Hernández-Figueroa, M. Zamboni-Rached, and E. Recami (Wiley, Hoboken, NJ, 2008).
  - [5] *Non-Diffracting Waves*, edited by H. E. Hernández-Figueroa, E. Recami, and M. Zamboni-Rached (Wiley, Berlin, 2014).
  - [6] *Structured Light and Its Applications: An Introduction to Phase-Structured Beams and Nanoscale Optical Forces*, edited by David L. Andrews (Academic Press, Cambridge, Mass., 2008).
  - [7] A. Ashkin, J. M. Dziedzic, J. E. Bjorkholm, and S. Chu, Observation of a single-beam gradient force optical trap for dielectric particles, *Opt. Lett.* **11**, 288 (1986).
  - [8] J. Arlt, V. Garcés-Chavez, W. Sibbett, and K. Dholakia, Optical micromanipulation using a Bessel light beam, *Opt. Commun.* **197**, 239 (2001).
  - [9] V. Garcés-Chavez, D. McGloin, H. Melville, W. Sibbett, and K. Dholakia, Simultaneous micromanipulation in multiple planes using a self-reconstructing light beam, *Nature* **419**, 145 (2002).
  - [10] M. P. MacDonald, L. Paterson, K. Volke-Sepulveda, J. Arlt, W. Sibbett, and K. Dholakia, Creation and manipulation of three-dimensional optically trapped structures, *Science* **296**, 1101 (2002).
  - [11] V. Garcés-Chavez, D. McGloin, M. J. Padgett, W. Dultz, H. Schmitzer, and K. Dholakia, Observation of the Transfer of the Local Angular Momentum Density of a Multiringed Light Beam to an Optically Trapped Particle, *Phys. Rev. Lett.* **91**, 093602 (2003).
  - [12] D. McGloin, V. Garcés-Chavez, and K. Dholakia, Interfering Bessel beams for optical micromanipulation, *Opt. Lett.* **28**, 657 (2003).
  - [13] D. G. Grier, A revolution in optical manipulation, *Nature* **424**, 810 (2003).
  - [14] M. Padgett and R. Bowman, Tweezers with a twist, *Nat. Photonics* **5**, 343 (2011).
  - [15] L. A. Ambrosio and M. Zamboni-Rached, Analytical approach of ordinary frozen waves for optical trapping and micromanipulation, *Appl. Opt.* **54**, 2584 (2015).
  - [16] G. Milne, K. Dholakia, D. McGloin, K. Volke-Sepulveda, and P. Zemánek, Transverse particle dynamics in a Bessel beam, *Opt. Express* **15**, 13972 (2007).
  - [17] V. Garcés-Chávez, D. McGloin, H. Melville, W. Sibbett, and K. Dholakia, Simultaneous micromanipulation

- in multiple planes using a self-reconstructing light beam, *Nature* **419**, 145 (2002).
- [18] J. Yin, Y. Zhu, W. Wang, Y. Wang, and W. Jhe, Optical potential for atom guidance in a dark hollow laser beam, *J. Opt. Soc. Am. B* **15**, 25 (1998).
- [19] V. E. Lembessis, A mobile atom in a Laguerre-Gaussian laser beam, *Opt. Commun.* **159**, 243 (1999).
- [20] J. Arlt, T. Hitomi, and K. Dholakia, Atom guiding along Laguerre-Gaussian and Bessel light beams, *Appl. Phys. B* **71**, 549 (2000).
- [21] D. P. Rhodes, G. P. T. Lancaster, J. Livesey, D. McGloin, J. Arlt, and K. Dholakia, Guiding a cold atomic beam along a co-propagating and oblique hollow light guide, *Opt. Commun.* **214**, 247 (2002).
- [22] E. Courtade, O. Houde, J. F. Clement, P. Verkerk, and D. Hennequin, Dark optical lattice of ring traps for cold atoms, *Phys. Rev. A* **74**, 031403 (2006).
- [23] J. Arlt, T. Hitomi, and K. Dholakia, Atom guiding along Laguerre-Gaussian and Bessel light beams, *Appl. Phys. B* **71**, 549 (2000).
- [24] E. G. P. Pachon, M. Zamboni-Rached, A. H. Dorrah, M. Mojahedi, M. R. R. Gesualdi, and G. G. Cabrera, Architecting new diffraction-resistant light structures and their possible applications in atom guidance, *Opt. Express* **24**, 25403 (2016).
- [25] T. A. Planchon, L. Gao, D. E. Milkie, M. W. Davidson, J. A. Galbraith, C. G. Galbraith, and E. Betzig, Rapid three-dimensional isotropic imaging of living cells using Bessel beam plane illumination, *Nat. Methods* **8**, 417 (2014).
- [26] A. H. Dorrah, M. Zamboni-Rached, and M. Mojahedi, Controlling the topological charge of twisted light beams with propagation, *Phys. Rev. A* **93**, 063864 (2016).
- [27] L. Allen and M. Padgett, Equivalent geometric transformations for spin and orbital angular momentum of light, *J. Mod. Opt.* **54**, 487 (2007).
- [28] D. L. Andrews, L. C. D. Romero, and M. Babiker, On optical vortex interactions with chiral matter, *Opt. Commun.* **237**, 133 (2004).
- [29] F. Araoka, T. Verbiest, K. Clays, and A. Persoons, Interactions of twisted light with chiral molecules: An experimental investigation, *Phys. Rev. A* **71**, 055401 (2005).
- [30] V. Chavez, D. McGloin, M. J. Padgett, W. Dultz, H. Schmitzer, and K. Dholakia, Observation of the Transfer of the Local Angular Momentum Density of a Multiringed Light Beam to an Optically Trapped Particle, *Phys. Rev. Lett.* **91**, 093602 (2003).
- [31] *Paraxial Light Beams with Angular Momentum*, edited by A. Bekshaev and M. Soskin (Nova Science Publishers, New York, 2008).
- [32] T. A. Vieira, M. R. R. Gesualdi, and M. Zamboni-Rached, Frozen waves: Experimental generation, *Opt. Lett.* **37**, 2034 (2012).
- [33] T. A. Vieira, M. R. R. Gesualdi, M. Zamboni-Rached, and E. Recami, Production of dynamic frozen waves: Controlling shape, location (and speed) of diffraction-resistant beams, *Opt. Lett.* **40**, 5834 (2015).
- [34] M. Corato Zanarella and M. Zamboni-Rached, Electromagnetic frozen waves with radial, azimuthal, linear, circular, and elliptical polarizations, *Phys. Rev. A* **94**, 053802 (2016).
- [35] M. Zamboni-Rached and M. Mojahedi, Shaping finite-energy diffraction- and attenuation-resistant beams through Bessel-Gauss beam superposition, *Phys. Rev. A* **92**, 043839 (2015).
- [36] A. H. Dorrah, M. Zamboni-Rached, and M. Mojahedi, Generating attenuation-resistant frozen waves in absorbing fluid, *Opt. Lett.* **41**, 3702 (2015).
- [37] Victor Arrizón, Optimum on-axis computer-generated hologram encoded into low-resolution phase-modulation devices, *Opt. Lett.* **28**, 2521 (2003).
- [38] Victor Arrizón, Guadalupe Méndez, and David Sánchez-de-La-Llave, Accurate encoding of arbitrary complex fields with amplitude-only liquid crystal spatial light modulators, *Opt. Express* **13**, 7913 (2005).
- [39] H. Rubinsztein-Dunlop *et al.*, Roadmap on structured light, *J. Opt.* **19**, 013001 (2017).
- [40] R. R. Gattass and E. Mazur, Femtosecond laser micro-machining in transparent materials, *Nat. Photonics* **2**, 219 (2008).
- [41] J. A. Dharmadhikari, A. K. Dharmadhikari, A. Bhatnagar, A. Mallik, P. Chandrakanta Singh, R. K. Dhaman, K. Chalapathi, and D. Mathur, Writing low-loss waveguides in borosilicate (BK7) glass with a low-repetition-rate femtosecond laser, *Opt. Commun.* **284**, 630 (2011).
- [42] V. Zambon, N. McCarthy, and M. Piché, Fabrication of photonic devices directly written in glass using ultrafast Bessel beams, *Proc. SPIE* **7099**, 70992J (2008).
- [43] M. K. Bhuyan, F. Courvoisier, P.-A. Lacourt, M. Jacquot, L. Furfaro, M. J. Withford, and J. M. Dudley, High aspect ratio taper-free microchannel fabrication using femtosecond Bessel beams, *Opt. Express* **18**, 566 (2010).
- [44] Federica Cattani, Arkady Kim, Mietek Lisak, and Dan Anderson, Interactions of electromagnetic radiation with Bose-Einstein condensates: Manipulating ultra-cold atoms with light, *Int. J. Mod. Phys. B* **27**, 1330003 (2013).